FEEDBACK CONTROL OF A CIRCULAR CYLINDER WAKE IN EXPERIMENT AND SIMULATION (INVITED)

Stefan Siegel*, Kelly Cohen**, Tom McLaughlin†

Department of Aeronautics
U.S. Air Force Academy, Colorado Springs, CO 80840, USA

Abstract

The effect of feedback flow control on the wake of a circular cylinder at a Reynolds number of 100 is investigated in both water tunnel experiment and direct numerical simulation. Our control approach uses a low dimensional model based on proper orthogonal decomposition (POD). The controller applies linear proportional and differential feedback to the estimate of the first POD mode. The range of validity of the POD model is explored in detail. Actuation is implemented as displacement of the cylinder normal to the flow. We demonstrate that the threshold peak amplitude below which the control actuation ceases to be effective is in the order of 5% of the cylinder diameter.

The closed loop feedback simulations explore the effect of both fixed phase and variable phase feedback on the wake. While fixed phase feedback is effective in reducing drag and unsteady lift, it fails to stabilize this state once the low drag state has been reached. Variable phase feedback, however, achieves the same drag and unsteady lift reductions while being able to stabilize the flow in the low drag state. In the low drag state, the near wake is entirely steady, while the far wake exhibits vortex shedding at a reduced intensity. We achieved a drag reduction of close to 90% of the vortex-induced drag, and lowered the unsteady lift force by the same amount.

Introduction

Two-dimensional bluff body wakes have been investigated for quite some time. In a two-dimensional cylinder wake, self-excited oscillations in the form of periodic shedding of vortices are observed above a critical Reynolds number of approximately 47. This behavior is referred to as the von Kármán Vortex Street. According to Williamson[1], the regime of laminar vortex shedding extends to a Reynolds number of approximately 180, before three-dimensional instabilities occur. This is the Reynolds number regime that we target in this investigation. However, the Kármán vortex street as the fundamental feature of this type of wake flow is sustained to very large Reynolds numbers (on the order of millions). Therefore the lessons learned at low Reynolds numbers will still be applicable to applications of practical interest at much higher Reynolds numbers. Conversely, it would be impossible to control the flow at high Reynolds numbers without being able to successfully do this at low Reynolds numbers.

The nonlinear oscillations of the vortex street lead to some undesirable effects associated with unsteady pressures such as fluid-structure interactions[2] and lift/drag fluctuations[3]. Also, the vortices themselves greatly increase the drag of the bluff body, compared to the steady wake that can be observed at lower Reynolds numbers. Monkewitz[4] showed that the von Kármán Vortex Street is the result of an absolute, global instability in the near wake of the cylinder. Further downstream the flow is convectively unstable. This absolute instability is causing the flow to behave as a self sustained oscillator, with internal positive feedback leading to temporal amplification of the oscillation by the recirculation region downstream of the cylinder.

Many attempts to improve the unsteady vortex street have been made. When active open loop forcing of the wake is employed, the vortex shedding in the wake can be locked in phase to the forcing signal[5]. While these findings suggest that the dominant structures in the flow field can be influenced by the forcing, it also strengthens the vortices, and, consequently increases the mean drag as well as unsteady lift fluctuations. Different forc-

* Assistant Research Associate, Member
** Visiting Researcher, Member
† Research Associate, Associate Fellow

ing methods are effective in influencing the behavior of the flow. Acoustic excitation of the wake, longitudinal, lateral or rotational vibration of the cylinder model, and alternate blowing and suction at the separation points[5] have been used. Using these methods, the flow exhibits regions of lock-in and non-lock-in. Koopmann[6] experimentally investigated these regions, and found that the lock-in frequency range depends on the forcing amplitude. The higher the forcing amplitude, the larger the frequency band for which he could achieve lock-in. Additionally, even at the natural vortex shedding frequency, he found a minimum threshold amplitude that was needed for lock-in to occur.

All of these open loop forcing methods have not been shown to reduce the drag, independent of frequency and amplitude employed. The only exceptions are situations where the separation point location is shifted. It should be noted that the geometry of a circular cylinder lends itself to active control methods that target the separation point location of the flow rather than the absolute instability of the wake itself. Using methods like periodic blowing and suction on the cylinder surface in a fashion similar to that employed on the suction side of airfoils, the separation point can be moved aft which in turn will lead to a narrower wake. A narrower wake will exhibit improved instability characteristics, in addition to lower drag due to a lower velocity deficit in and by itself. This effect can be observed in the natural cylinder wake during the "drag crisis", when boundary layer transition occurs upstream of the separation point, and the resulting turbulent boundary layer shifts the separation point downstream. Thus feedback control investigations using periodic blowing and suction like those employed by Min and Choi[7] actually employ two flow control techniques simultaneously, namely separation control and wake stabilization due to feedback. It is difficult if not impossible to judge what portion of the improvement is due to either of these techniques in their simulations.

The only way of suppressing the self-excited flow oscillations without altering the mean flow is by the incorporation of active closed-loop flow control[8]. Traditionally, several fundamentally different approaches to achieve feedback flow control have been employed. The mathematically driven approach to develop a control scheme is hampered by the complexity of the governing Navier Stokes equations. In order to tackle this complexity, one needs to make simplifying assumptions. At this point, the assumptions made in simplifying the equations have often rendered the results inapplicable to real life experiments, like in the investigations of Li and Aubry[9], where the controller needs to be activated at zero flow velocity in order to be able to stabilize the wake. This is an example of how assumptions made in the controller derivation may render the controller incapable of dealing with the non-simplified physics of the flow field. If no simplifications or assumptions are made, however, the resulting control algorithm (if it can be derived at all with today's computing capabilities) is often too complex to be implemented in real time. This is particularly true for certain optimum control approaches as they are being investigated in Bewley and Trenchea[10].

On the other hand, approaching the controls problem using an experimental / empirical approach without any modeling of the physics of the flow does not yield good results either. Experimental studies conducted by Roussopulos[2] show that a linear proportional feedback control based on a single sensor feedback is able to delay the onset of the wake instability only slightly, rendering the wake stable at Re about 20% higher than the unforced case. Roussopulos reports that above Re = 60, a single-sensor feedback may suppress the original mode but destabilizes one of the other modes. Therefore, better control strategies are needed to stabilize the wake at Reynolds numbers of technical interest.

The solution to this problem lies in the development of a low order model of the flow. The model can be used both for controller development, as well as flow field state estimation. Ideally, it reduces the complexity of the governing Navier Stokes equations to a level that the model can be implemented in real time, while still capturing the important physics of the flow. Gillies[11] pioneered the application of this technique to cylinder wakes by developing a low dimensional model of the cylinder wake at a Reynolds number of 100. Cohen et al.[12] have shown that using this model, the cylinder wake model flow can be successfully controlled using a relatively simple linear control approach based on the most dominant mode only.

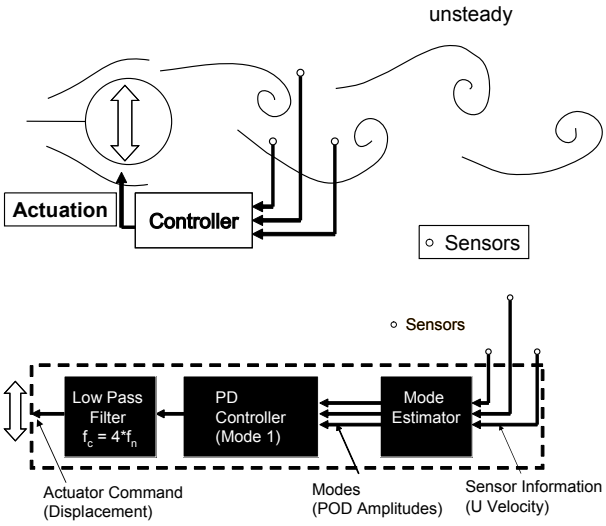

FIGURE 1 Feedback Control Setup

The goal of this paper is to apply the approach developed by Cohen et al.[12] to a full Navier Stokes simulation of the flow field, as well as a water tunnel experiment. In both simulation and experiment a limited number of sensors are used to estimate the state of the flow which is characterized using a low dimensional model. The controller then acts on the flow state estimates in order to determine the actuator displacement (Figure 1 shows the overall setup of this experiment).

Numerical Methods

CFD Model

For the numerical simulations, Cobalt Solutions' Cobalt solver V.2.02 was used. This code can operate in many different modes using various turbulence models. However, for the present investigation it was used as a direct Navier Stokes solver with second order accuracy in time and space. Cobalt operates on unstructured grids, for all investigations an unstructured two-dimensional grid with 63700 Nodes / 31752 Elements was used, see Figure 2. The grid extended from -16.9 cylinder diameters to 21.1 cylinder diameters in the x (streamwise) direction, and ±19.4 cylinder diameters in y (flow normal) direction.
Other pertinent simulation parameters:

- Reynolds Number (Re) = 100
- Mean flow, U= 34 m/s
- Damping Coefficients: Advection = 0.01; Diffusion = 0.00
- 32 Iterations for matrix solution scheme
- 3 Newtonian sub-iterations
- Non-dimensional time step $\Delta t^* = \Delta t*U/D=0.05$
- Time step, Δt = 0.00147 s
- Vortex shedding frequency 5.55 Hz

The simulation was triggered by skewing the incoming mean flow by α = 0.5 degrees in order to introduce an initial perturbation. An important issue concerning the validity of the CFD model needs to be addressed before using the data. For validation of the unforced cylinder wake CFD model at Re = 100, the resulting value of the mean drag coefficient, c_d, will be compared to experimental and computational investigations reported in the literature. At Re = 100, experimental data, reported by Oertel[13] and Panton[14] point to c_d values ranging from 1.26 to 1.4. Furthermore, Min and Choi[7] report on several numerical studies that obtained drag coefficients of 1.35 and 1.337. The COBALT CFD model, used in this effort results in a c_d =1.35 at Re = 100, which compares well with the reported literature. Another important benchmark parameter is the non-dimensional vortex shedding frequency, the Strouhal number (St) for the unforced cylinder wake. Experimental results at Re = 100, presented by Williamson,[1] show Strouhal numbers ranging from 0.163 to 0.166. The Strouhal number obtained from the COBALT CFD model used in this effort is St = 0.163 at Re = 100 which compares well with the reported literature.

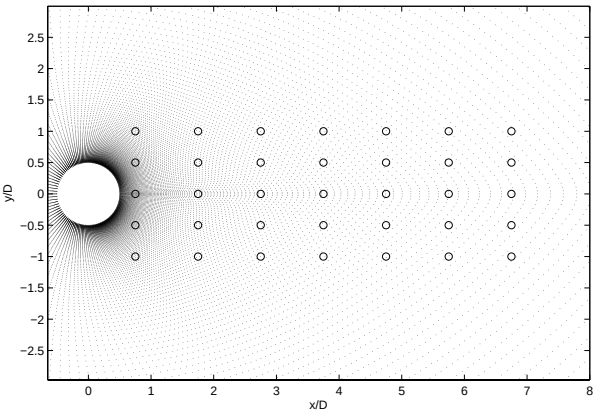

FIGURE 2. Computational grid (dots) and sensor locations (circles).

The simulations were performed on a Beowulf Linux cluster consisting of 64 Pentium III processors operating at 1 Ghz. When running on 8 processors, typically a time step took on the order of 6 s to compute. Employing larger number of processors yielded unproportional small improvements in execution time, due to network and disk access overhead for saving the results at the end of each time step.

POD Modeling and Estimation

Feasible real time estimation and control of the cylinder wake may be effectively realized by reducing the model complexity of the cylinder wake as described by the Navier-Stokes equations, using POD techniques. POD, a nonlinear model reduction approach is also referred to in the literature as the Karhunen-Loeve expansion[15]. The desired POD model contains an adequate number of modes to enable modeling of the temporal and spatial characteristics of the large-scale coherent structures inherent in the flow.
In this effort, the method of "snapshots" introduced by Sirovich[16] is employed to generate the basis functions of the POD spatial modes from the numerical solution of the Navier-Stokes equations obtained using COBALT. In all 200 snapshots were used equally spaced at 0.00735 seconds apart. The time between snapshots is five times the simulation time step. The snapshots were taken after ensuring that the cylinder wake reached steady state. Only the U velocity component (in the direction of the mean flow) was used for POD decomposition in this effort. This decision was made in order to be able to esti-

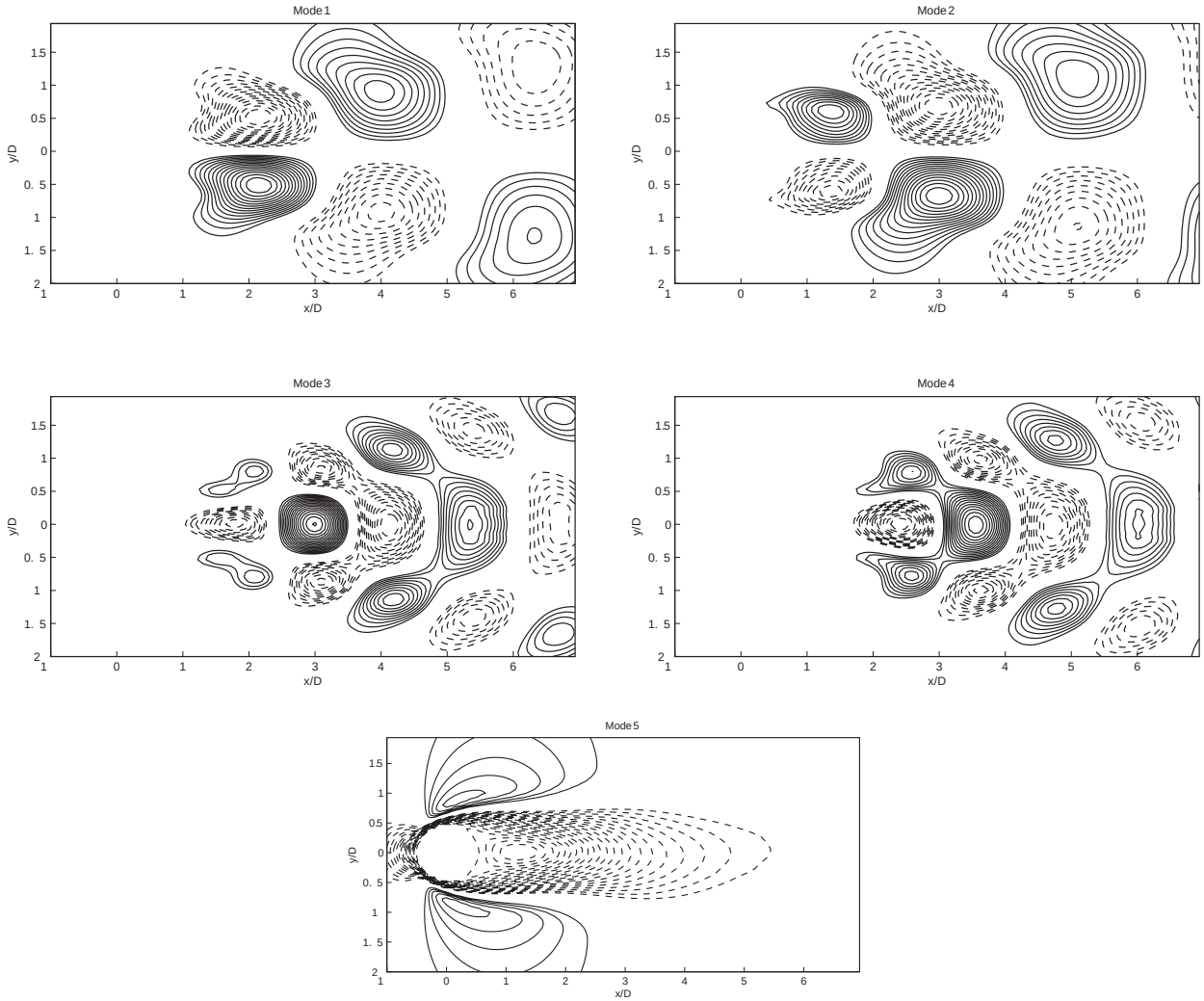

FIGURE 3. Eigenfunctions of the 5 Mode POD model based on CFD data at Re = 100, using the U velocity component as input for the POD decomposition. Solid lines are positiv, dashed lines negative isocontours.

mate the mode amplitudes based on sensor information, which in our experiment will yield the U and V component of velocity. Since the change in mean flow distribution is an important quantity, we chose the U velocity component over the V velocity component. We found that more than 99.98% of the kinetic energy of the flow lies in the first eight modes, with more than 90% in the first four modes. An important aspect of reduced order modeling concerns truncation: how many modes are important and what are the criteria for effective truncation?

The answers to the above questions have been addressed by Cohen et al.[12] This effort showed that control of the POD model, of the von Kármán vortex street in the wake of a circular cylinder at Re = 100, is enabled using just the first mode. Furthermore, feedback based on the first mode alone suppressed all the other modes in the four mode POD model, indicating that higher order modes derive from the fundamental modes. In view of this result, truncation of the POD model took place after the first four modes, which contain more than 93.5% of the total amount of energy. At this point, it is imperative to note the difference between the number of modes required to reconstruct the flow and the number of modes required to control the flow. In this effort, we are interested in estimating only those modes required for closed-loop control. On the other hand, an accurate reconstruction of the velocity field based on a low-dimensional model may be obtained using between 4-8 modes.[17] The POD algorithm was applied to the fluctuating velocity component in the direction of the flow as described in Equation (1). The decomposition of this component of the velocity field is as follows:

$$\tilde{u}(x, y, t) = U(x, y) + u(x, y, t) \qquad (1)$$

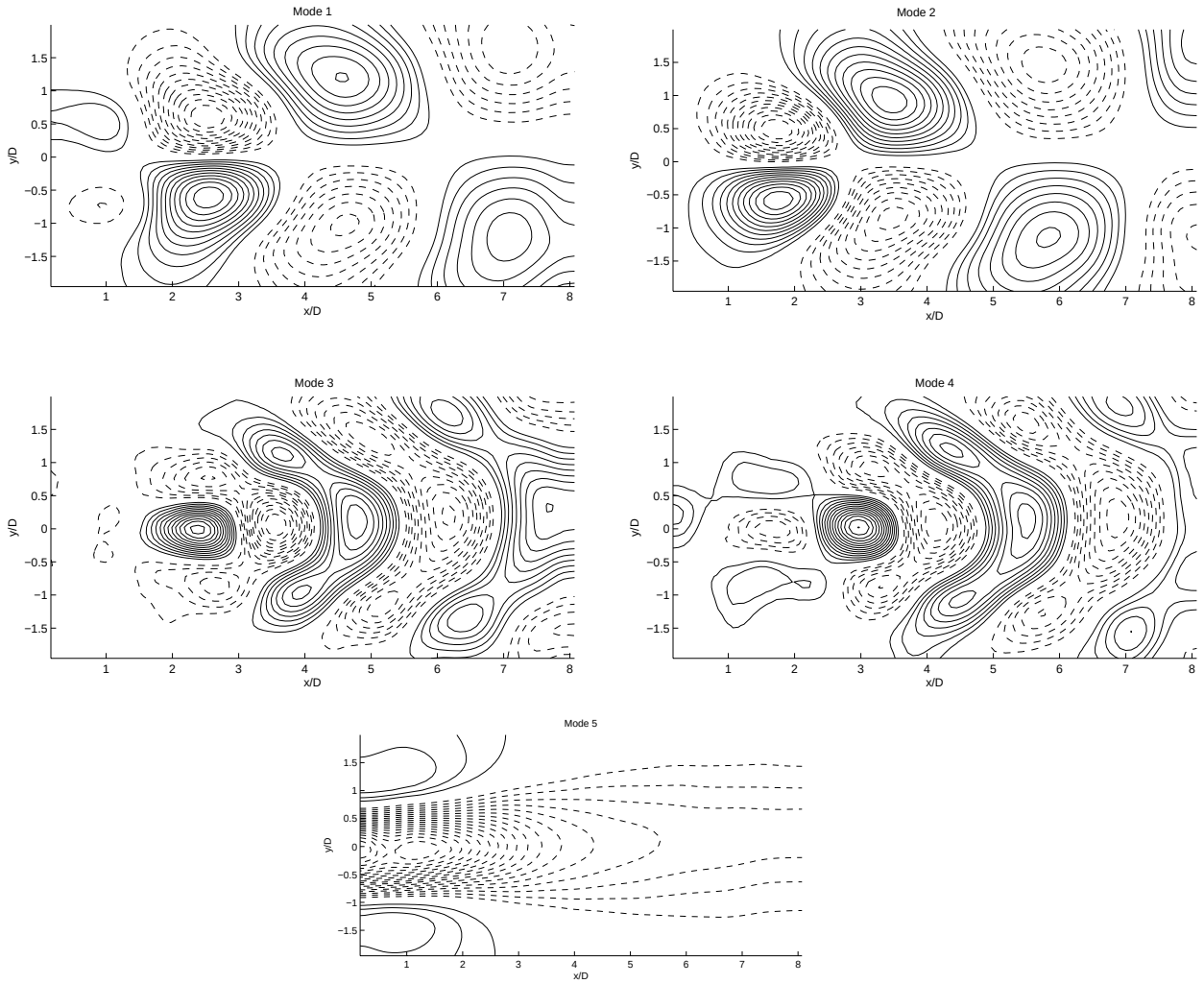

FIGURE 4. Eigenfunctions of the 5 Mode POD model based on water tunnel data at Re = 120,, using the U velocity component as input for the POD decomposition. Solid lines are positiv, dashed lines negative isocontours.

where U[m/s] denotes the mean flow velocity and u[m/s] is the fluctuating component that may be expanded as:

$$u(x, y, t) = \sum_{k=1}^{n} a_k(t)\phi_i^{(k)}(x, y) \qquad (2)$$

where $a_k(t)$ denotes the time-dependent coefficients having units of m/s and $\phi(x, y)$ represent the non-dimensional spatial eigenfunctions (see Fig. 3 and 4) determined from the POD procedure. The velocity field snapshots may be obtained from a CFD simulation or from PIV (particle image velocimetry) measurements. Since our goal is to conduct both CFD simulations and water tunnel experiments employing closed loop feedback, we applied the above POD procedure to both experimental and simulation data. The spatial eigenfunctions for both cases, albeit at slightly different Reynolds numbers, are shown in Figures 3 and 4, respectively. Both experiment and simulation show qualitatively good agreement. Shown are the first four modes of the POD decomposition, plus a 5th mode that was derived by subtracting the mean freestream velocity from the mean flow distribution of the unforced flow field. This mode was found to be necessary to obtain an estimate of the effect of feedback flow control onto the mean flow. It is being used to both estimate the effectiveness of the controller, as well as allow for gain scheduling to account for changes in the flow receptivity to forcing in a real time fashion. Additionally, Noack et al.[18] have shown that adding a similar mode to account for changes in the mean flow greatly improves the ability of the model to account for transient effects in the flow field. We will show the correlation between the mean flow mode and the wake drag in the following section.

Once the spatial POD eigenfunctions have been derived, the corresponding time-dependent coefficients $a_k(t)$, or

Mode amplitudes, need to be calculated. For this, two different schemes are reported in literature. Most often a Galerkin projection is used, which involves projecting the spatial eigenfunctions onto the Navier Stokes equations. This process involves spatial derivatives of the snapshots, which are, particularly in the case of experimental data, inherently sensitive to noise. Gillies[8] used a simple least squares fit, which we found to be much more robust. While we employ the least square fit in the CFD simulations, the experiment will make use of linear stochastic estimation (LSE) in order to estimate the mode amplitudes in real time. LSE is deterministic in terms of computing time, while least square fitting is not. Thus LSE is a much better choice for real time implementation.

For the feedback controlled runs, the CFD solver writes sensor information at requested (x, y) locations in the flow to a file after calculating a time step, and then waits for an external control algorithm to update the file with the new cylinder displacement for the next time step. The sensor grid employed for all simulations is shown in Figure 2 and employs a total of 35 sensors in the near wake of the cylinder. The main advantage of this sensor grid over others investigated is in its ability to provide a global estimate of the mode amplitudes that shows little error compared to using all grid points. This holds true both for the unforced case as well as the feedback controlled cases. Typical errors are negligible in phase and less than 5 % in amplitude.

While no extensive efforts to optimize the sensor locations was undertaken, we compared a localized sensor field with 35 sensors between x/D = 0.75 and x/D = 1.75 to the configuration shown in Figure 2. While both grids performed equally well in estimating the unforced flow field, for the feedback control runs the local grid develops large phase and amplitude errors as soon as the flow responds to the forcing. With this finding we decided to use the distributed sensor field shown in Figure 2.

Controller

The Cobalt CFD solver has the ability to perform rigid body motion of a given grid. This feature was used to perform both time periodically forced and feedback controlled simulations with one degree of freedom. For all investigations, only displacement of the cylinder in flow normal (y) direction was employed for forcing the flow. The control algorithm acts on the estimate of the Mode 1 amplitude only. This design decision was made based on our earlier investigations controlling a low dimensional model of the flow. For the low dimensional model, proportional gain applied to Mode 1 only was sufficient to suppress vortex shedding. Since our CFD simulations require a filter to avoid feeding back of small amounts of noise, we employed a Proportional and Differential (PD) feedback control strategy:

$$y_{cyl} = K_p \cdot a_1 + K_d \cdot \frac{da_1}{dt} \qquad (3)$$

Instead of directly specifying the K_p and K_d gains, these can be expressed in terms of an overall gain K and a phase advance φ:

$$K_p = K \cdot \cos(\varphi)$$
$$K_d = \frac{K \cdot \sin(\varphi)}{2\pi f} \qquad (4)$$

With f being the vortex shedding frequency.

Physically, the control algorithm was implemented in Matlab on a separate PC running Windows. It interfaced to the Beowulf cluster running Cobalt using Windows file sharing through Samba in order to read the sensor information and update the cylinder displacement.

Results

Before closed loop feedback flow control is employed, it is important to investigate the dynamics of the unforced flow field in detail. Equally important, the effect of open loop forcing needs to be understood, since the receptivity of the flow to forcing will manifest itself in these investigations. The following section will outline the results of these investigations, and also show the limitations of the type of forcing employed as well as the limits of the flow improvements that may be obtained using feedback control.

The following two sections will highlight a few select cases of the unforced flow, open loop forced flow and feedback controlled flow. Two different kinds of feedback control were employed, one using a fixed set of proportional and differential gains, and one set where the gains were varied depending on the change in the mean flow. The latter is usually referred to as a gain scheduling scheme.

Unforced Wake Properties

In a CFD simulation, the flow field is started abruptly at time zero. Figure 5 shows the evolution of the flow field after this startup. The flow evolves from a Stokes-type streamline pattern at t = 0 s through a steady wake with two closed recirculation bubbles at t = 0.4 s into the unsteady von Kármán Vortex Street observed at t = 2.94 s. During this startup, the flow reaches a state of minimum drag at t =0.7 s. This minimum drag coincides with a maximum amplitude of mode 5 as well as a maximum

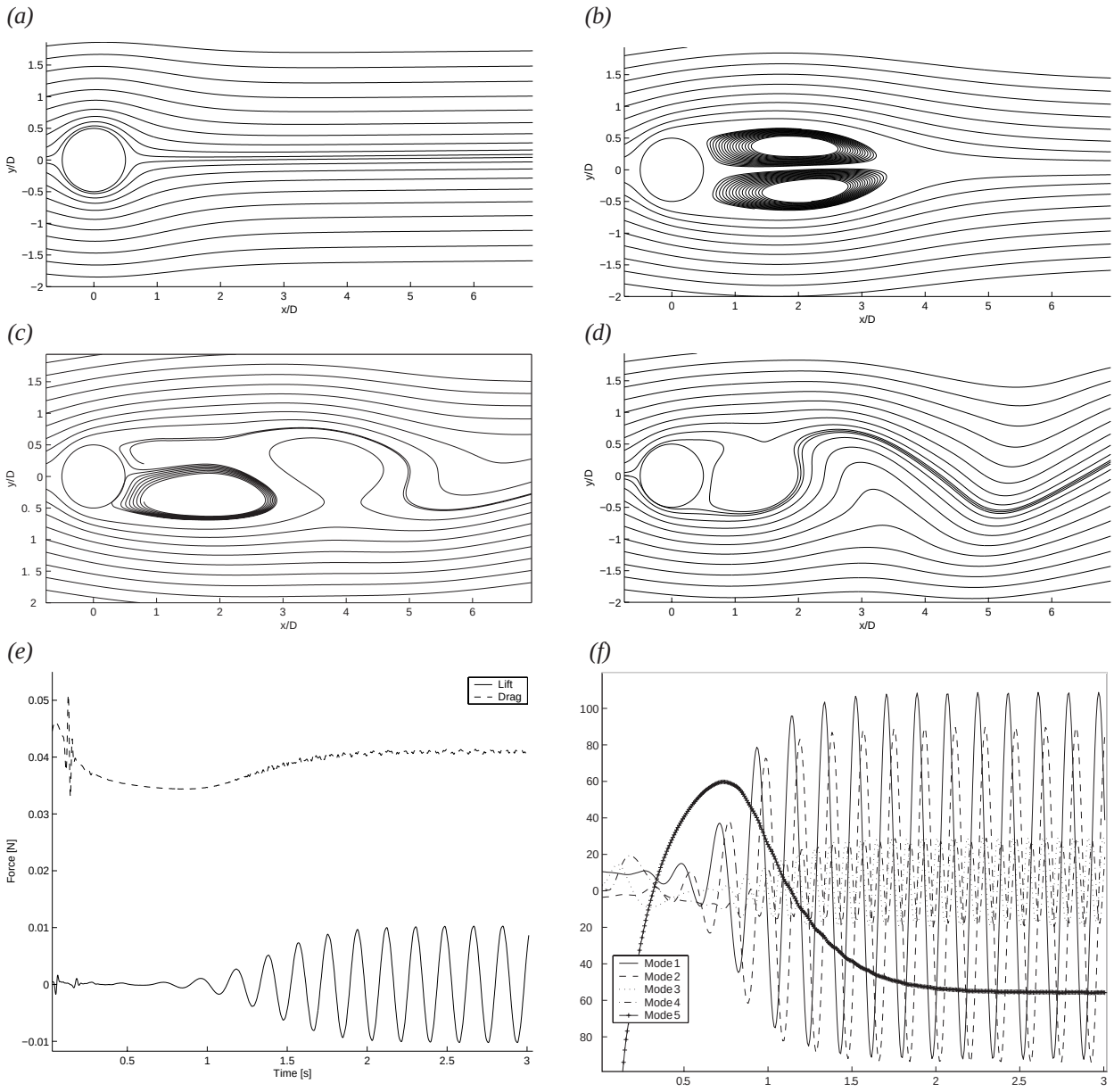

FIGURE 5. (a)-(d) Instantaneous streamlines at t = 0.0, 0.4, 0.7 and 3.0 seconds after startup of the simulation. (e) lift and drag during startup of the simulation. (f) Mode amplitudes during startup of the simulation, for spatial mode distributions see Figure 4.

mean recirculation zone length with the downstream end of the recirculation zone located at x/D = 5.4 (not depicted). It is worth noting that the minimum drag does not coincide in time with the steady wake as one might expect, but rather with a vortex shedding pattern with a very large wavelength, as shown in Figure 5 (c). The total drag in this situation is about 16 % less than in the steady state vortex shedding situation. Thus one may argue that a feedback control scheme aiming to suppress the vortex shedding may be able to recover up to this portion of the total drag, at best. We refer to this portion of the overall drag force as the ***vortex induced drag***, since it is caused by the vortex shedding in the unsteady wake flow. It is a portion of the pressure drag. After about 2 seconds after the startup of the simulation, the wake approaches a time periodic vortex shedding state. The mean recirculation zone ends at x/D = 1.9 in this flow state.

Open Loop Forced Wake Properties

The cylinder wake flow can be forced in an open loop fashion using sinusoidal displacement of the cylinder with a given amplitude and frequency. Koopman[6] investigated

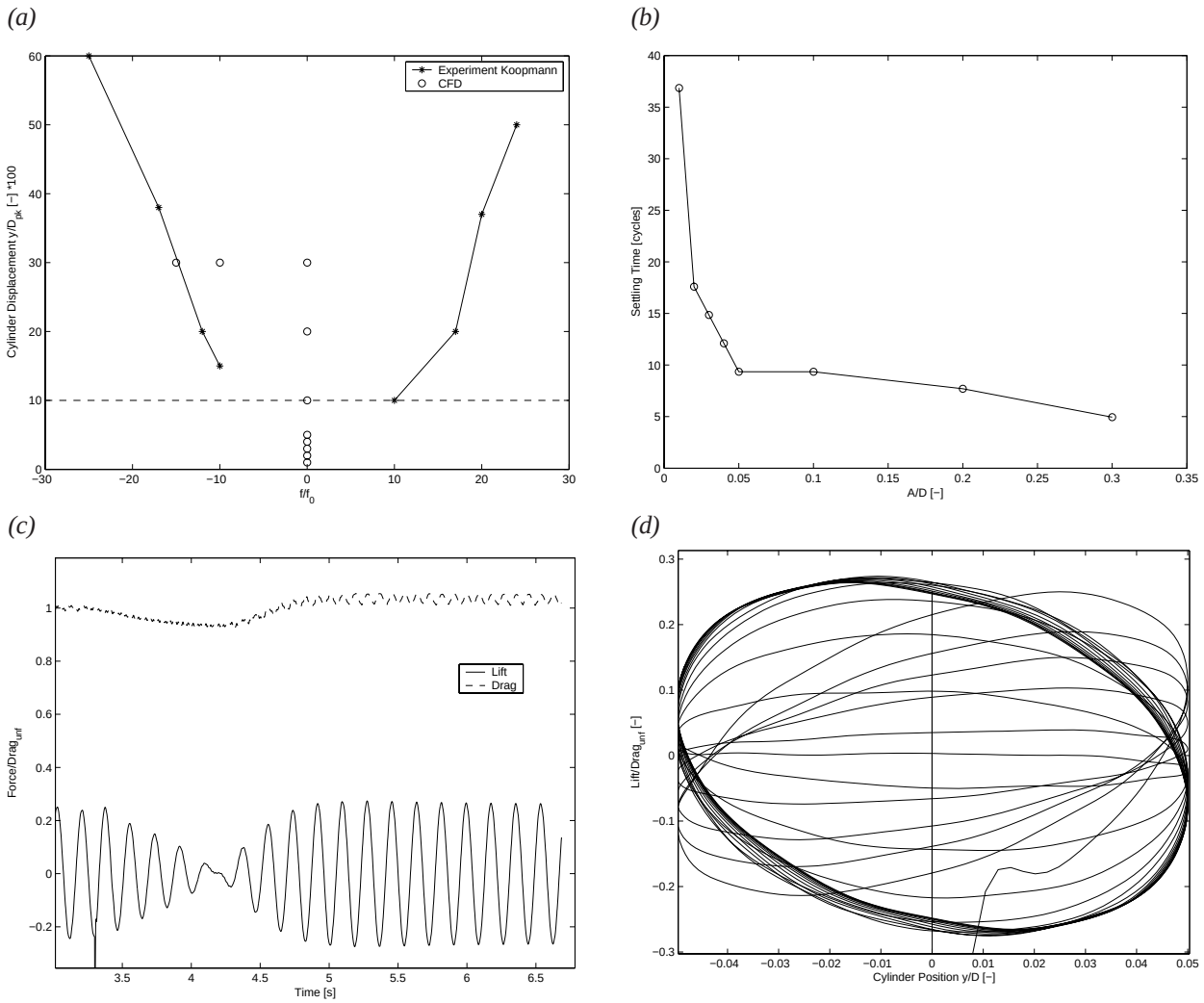

FIGURE 6. (a) Lock-in region adapted from Koopman (1966) (b) Settling time for different forcing amplitudes using sinusoidal forcing at the natural shedding frequency. (c-d) Sinusoidal forcing at the natural frequency using an amplitude of 5% of the cylinder diameter (c) Lift and Drag (d) Phase plot lift force vs. cylinder motion.

the response of the flow to this type of forcing in a wind tunnel experiment. He found a region around the natural vortex shedding frequency where he could achieve "lock-in", which is characterized by the wake responding to the forcing by establishing a fixed phase relationship with respect to the forcing. The frequency band around the natural vortex shedding frequency for which lock-in may be achieved is amplitude dependent, as shown in Figure 6(a). In general, the larger the amplitude, the larger the frequency band for which lock-in is possible. However, a threshold amplitude exists below which the flow will not respond to the forcing any more. In Koopman's experiment, this amplitude was at 10% peak displacement of the cylinder.

We resampled the lock-in region in the CFD simulation at select amplitude and frequency pairs shown in Figure 6(a). The simulations activated the forcing always at the same time, 3.3 seconds after the start of the simulation, which resulted in the forcing being 180 degrees out of phase with the vortex shedding. A typical run resulting in lock-in is depicted in Figure 6(c) and 6(d). It can be seen that the flow field goes through a transient phase before lock-in is achieved after about 9 shedding cycles. After the transient a fixed phase relationship between forcing and vortex shedding is established, as shown in Figure 6(d). We refer to the time during which the flow adjusts to the forcing as the settling time. A scan through different forcing amplitudes was performed at the natural shedding frequency with amplitudes ranging from 1 to 30 % of the cylinder diameter. The settling times observed in these cases are shown in Figure 6(b). While the settling times are roughly constant down to a forcing amplitude of 5%, for smaller amplitudes a drastic increase in settling times can be observed. This manifests

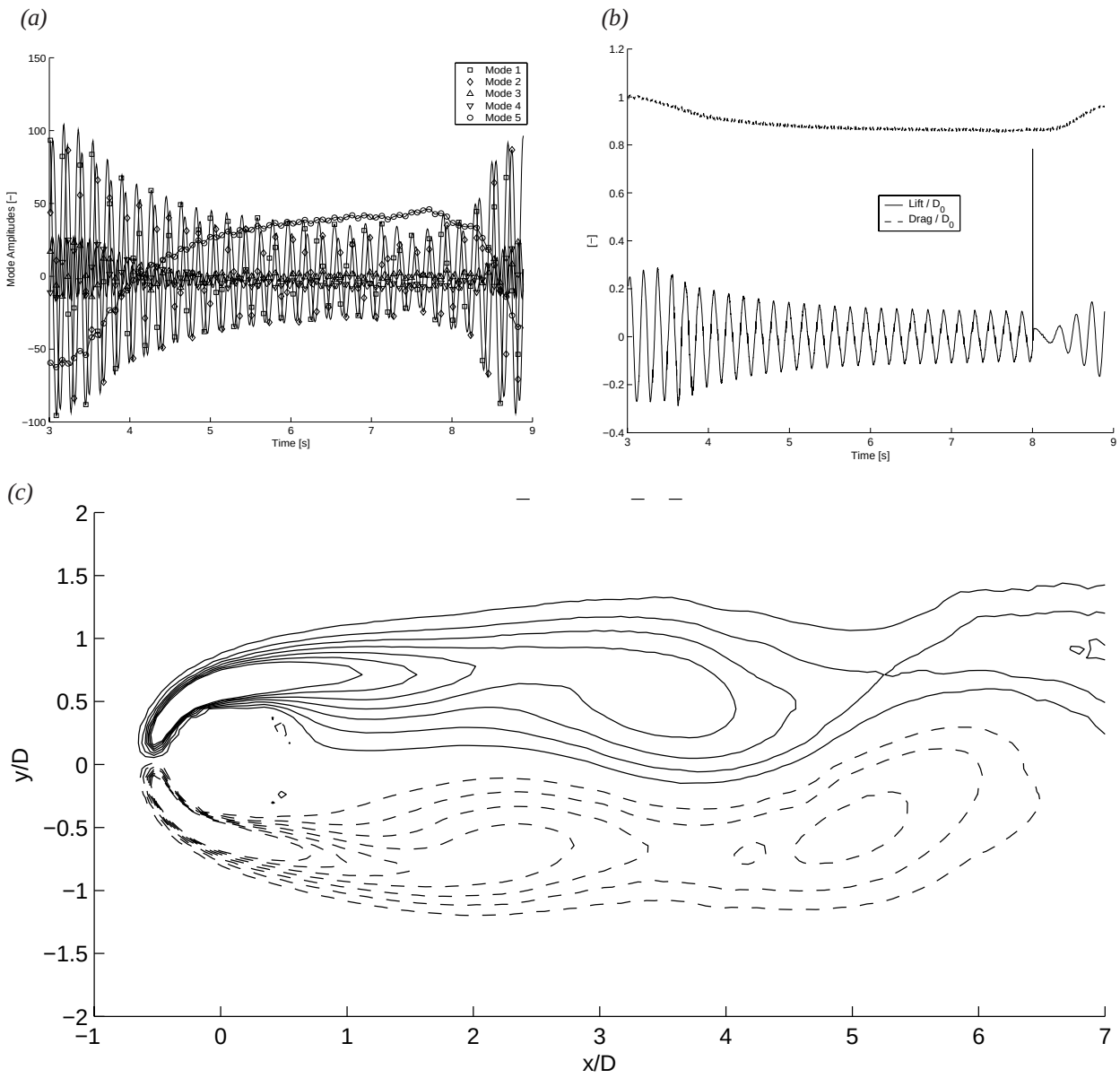

FIGURE 7. Linear feedback of Mode 1 with 30° Phase advance. The controller is activated at 3.03 s and deactivated at 8 s. (a) Mode Amplitudes (b) Cylinder Displacement and Frequency (c) Instantaneous Vorticity Contours at t = 6.5 s

the behavior observed by Koopman around 10% forcing amplitude, albeit shifted towards somewhat smaller amplitudes. There are two possible explanations for this. Koopman used spanwise coherence as an indicator for lock-in, which may occur at larger amplitudes than the local lock-in observed in our two-dimensional simulations. Additionally, his experiment was conducted in a wind tunnel environment which features more mean flow turbulence than the CFD simulations. This would also tend to increase the amount of forcing needed to overcome the turbulence and achieve lock-in.

Shifting the forcing frequency away from the natural shedding frequency yields a qualitatively different behavior, ultimately yielding a chaotic flow behavior at and beyond the lock-in limit according to Koopman. We were able to verify this behavior (results not shown).

The open loop forcing results have important implications for the closed loop feedback control runs. Since our POD model is based on unforced flow field data, it can only capture flow behavior that is phenomenologically similar to the unforced wake. In terms of the lock-in region, this flow behavior is encountered as long as the controller keeps the flow within the lock-in region. The

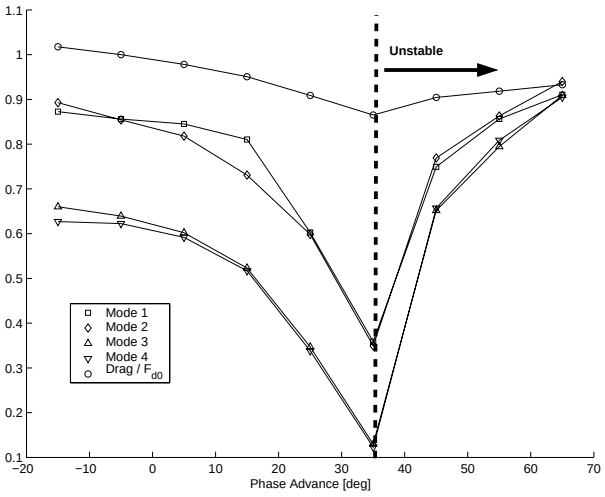

FIGURE 8. Mode Amplitudes and drag force for various phase advance angles.

chaotic behavior at off-natural frequencies is clearly not modeled in the POD modes. Also, more importantly, if the displacement of the cylinder becomes smaller than about 5% of the cylinder diameter, the flow will no longer be responsive to the forcing.

Fixed Phase Feedback

A series of simulations with different phase advance φ were conducted. The overall gain K was kept constant at a value that resulted in initial displacements of less than 15% of the cylinder diameter, in order to avoid strongly nonlinear effects that have been reported in literature at higher amplitudes. Qualitatively, the runs resulted in either an increase of the mode amplitudes or a reduction of the mode amplitudes. A case with a decrease in mode amplitudes is shown in Figure 7. During the control run, the global mode amplitude of Mode 1 decreases from a peak value of around 100 to a peak value of less than 40. This decrease in mode amplitude does not just apply to Mode 1, but also to Mode 2 and the two higher order modes. These findings are consistent with our experience in controlling a low order model of the flow[12], where a similar coupling between the modes could be observed. Considering the behavior of the unsteady lift and the drag (Figure 7b), a reduction in drag of about 14% of the unforced drag can be observed, while the unsteady lift is reduced by about 50 %. Comparing the drag reduction of 14% to the minimum drag encountered during startup of the CFD simulation, which is 16% less than the drag of the unforced flow field, we find that the simple feedback controller with a fixed gain and phase recovers more than 87% of the steady wake flow drag reduction. However, all of our fixed phase simulations that led to a drag reduction were not able to stabilize the flow at a low drag value. In Figure 7(a) at a time of 7.5 s, a reduction followed by an increase in mode amplitude can be observed. This is the first indication of the onset of an instability that will ultimately render the flow field chaotic, if the simulation is continued. Inspecting the cylinder displacement during this simulation (not shown), the onset of the instability coincides with a cylinder displacement that has just dropped below 5% of the cylinder diameter. Thus the onset of the instability coincides with the loss of flow response found in the periodically open loop forced runs discussed in the previous section. The instantaneous vorticity contours shown in Figure 7(c) show a wake flow where the vortices form further downstream of the cylinder, compared to the unforced flow shown in Figure 5(d). In the unforced flow, the vortices roll up between 1 and 2 diameters downstream of the cylinder, while in the feedback controlled situation the rollup occurs between 3 and 4 diameters downstream. As a result the reverse flow region is lengthened, from x/D = 1.9 in the unforced case to x/D = 4.3. Simultaneously with the lenghtening of the recirculation zone we observe a reduction in the vortex shedding frequency. The correlation between the shedding frequency and the reduction in drag is in qualitative agreement with the wake model proposed by Ahlborn et al.[19].

A summary of the effect of different amounts of fixed phase advance on both the mode amplitudes and the drag force is shown in Figure 8. While it is apparent that the largest drag and mode amplitude reductions are achieved for a phase advance of about 35 degrees, this phase advance is also unstable over longer time periods. The good correlation between the mode amplitude reduction and the drag reduction suggests a strong link between these quantities. Also, it can be seen that all mode amplitudes experience a proportional reduction which shows the coupling between the modes to be strong. It is also interesting to note that a zero degree phase advance has no impact on the drag.

With these findings on the impact of fixed phase feedback on the wake, an important question to be asked is if the wake can be stabilized at a low mode amplitude, and if so, how. An obvious parameter to adjust in order to achieve this is the gain of the controller. Increasing the gain leads to larger cylinder displacements, which would assure the ability to control the wake at small mode amplitudes. However, we found that larger gains do not stabilize the wake but rather lead to a low frequency oscillation and instability even when the cylinder displacements are kept above 5% of the cylinder diameter. The other parameter to be considered for adjustment is the phase of the feedback which we report on in the following section.

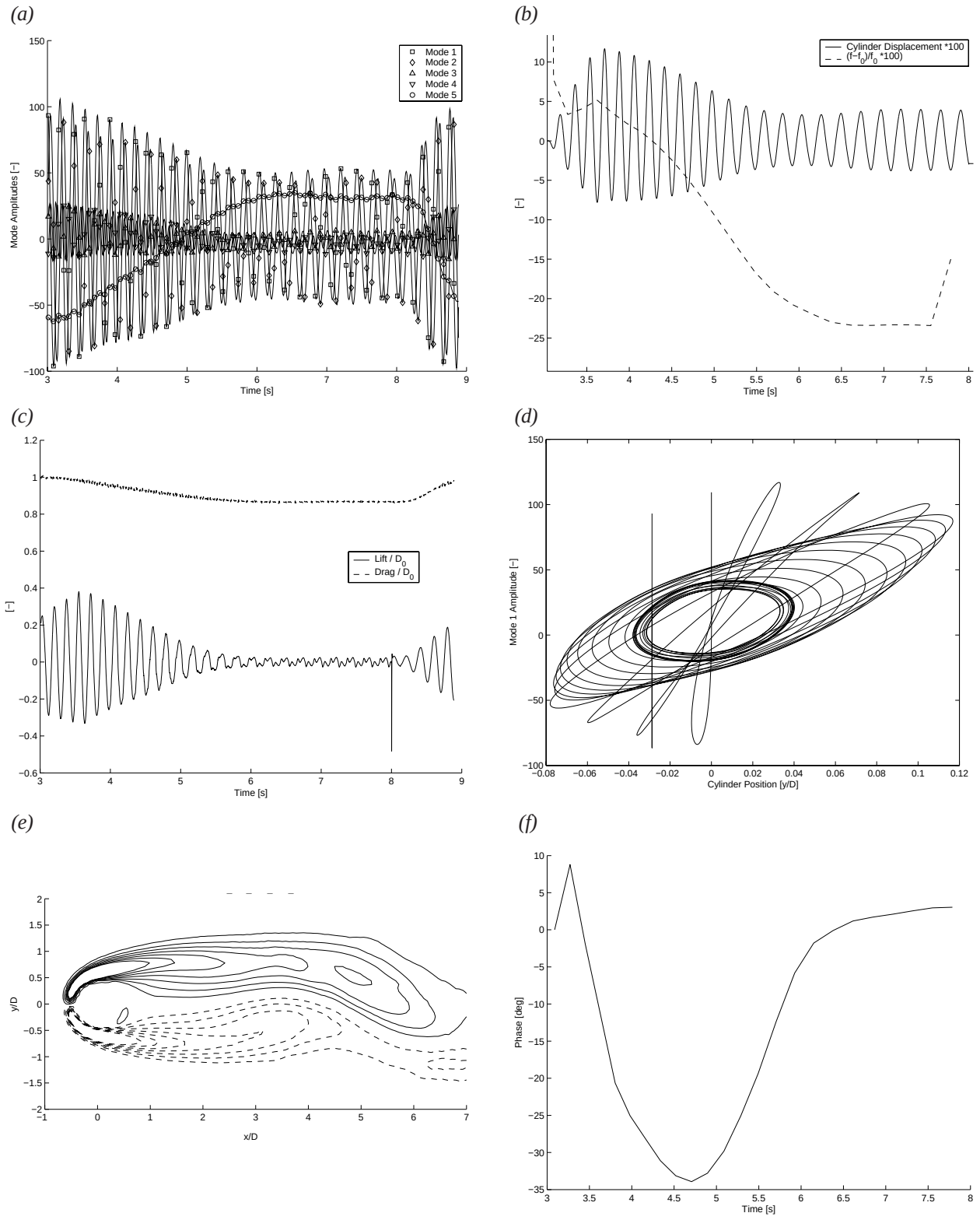

FIGURE 9. Linear feedback of Mode 1 with variable Phase advance. (a) Mode Amplitudes (b) Cylinder Displacement and Frequency (c) Lift and Drag (d) Phase between Cylinder Position and Mode 1 (e)Instantaneous Vorticity Contours at t=7.5 s (f) Phase advance during the run

Variable Phase Feedback

During an investigation into different sensor configurations, we used a sensor field with 35 sensors localized between x/D = 0.75 and x/D 1.75. As was later discovered, this sensor field developed a large estimation error with respect to the phase error of the Mode 1 estimate, when compared to an estimate based on the entire flow field, as shown in Figure 9 (f). Nonetheless, this phase error led to a stabilization of the wake at an overall drag reduction of about 15% with an unsteady lift amplitude reduction of 90%, compared to the unforced flow field. Inspecting the phase error, one can see that due to the effects of the local sensor field the phase advance is reduced to almost zero in the steady state case. This phase advance angle stabilizes the flow field at a low level of vortex shedding , with the recirculation length extended to x/D = 3.95, or more than twice the unforced length. While in the run shown in Figure 9 the phase advance was a result of the sensor placement, the same effect can be achieved using a global sensor field like the one shown in Figure 2 in combination with a variable phase advance based on the non - fluctuating Mode 5. Thus we find that a variable gain strategy that adjusts the feedback gains according to the change in the mean flow achieves better results than a fixed gain control approach.

Discussion

We used Proper Orthogonal Decomposition (POD) as a tool to process multiple sensor signals into a global estimate of the flow state. POD allows for stable global wake state estimate, enables multi sensor evaluation and eliminates artifacts of local sensing, i.e. sensing at nodes of the vortex street. It also allows for an accurate state estimate when the effect of the controller causes major changes both in the mean flow and the rms amplitudes of the fluctuating velocity components. However, we find it necessary to account for the changes in the mean flow by adding a mean flow mode to the model.

While we used only Mode 1 for closing the feedback loop, all the higher order POD modes experienced proportional reductions in mode amplitude. This suggests a strong coupling between all modes, and implies that the existence of the higher order modes is conditional on the presence of the fundamental modes. This confirms the results of our previous work[12].

While feedback control was able to stabilize the near wake of the cylinder, vortex formation still occurred further downstream. While the reasons for this are not entirely clear, we suggest several possible causes. The change in the mean flow caused by the controller lengthens the recirculation zone. This moves the vortex formation location further downstream and causes a reduction in both drag and rms lift force. While both of these effects are desired, the downstream shift in vortex formation location causes a larger spatial separation between the actuation, which remains at the cylinder, and the oscillations the actuator attempts to cancel. This requires both more actuation input, and also an adjustment in the actuation phase in order to account for the time a given disturbance takes to travel from the actuator to the vortex formation location. At the same time the disturbances caused by the actuator need to travel through a region of the flow which, while stabilized, is only stabilized within a narrow range of phase angles. If the far wake requires a phase angle for stabilization that at the same time destabilizes the near wake, a physical limit has been reached in terms of what can be achieved given the actuator location. This effect may limit the spatial range for which stabilization can be achieved with the current actuator setup.

Despite all these problems, we were able to suppress the oscillations in the near wake without actively modifying the mean flow or changing the separation point using for example momentum injection. Thus this effort shows that the cylinder wake flow can be improved in terms of drag and unsteady lift by feedback control. For this reason, one would expect the current control approach to be applicable to wake flows with fixed separation points, like the flow around a D- shaped cylinder. The same cannot be said for approaches that aim at moving the separation point aft, for example by tripping the boundary layer or using blowing and suction upstream of the separation point to delay separation.

In parallel with this paper, Gerhard et al.[20] also employ a low order model based approach to control the circular cylinder wake. While details of the low order model, estimation technique and control algorithm employed are different from our approach, the qualitative effects of the control on the flow field appear to be very similar. This indicates that the limitations encountered in both of our control approaches may be inherent to actuation authority - both approaches use a localized actuation in a small portion of the flow field - and inherent to the physics of the flow field itself.

Overall, we were able to reduce the effect of vortex shedding on both the unsteady lift and the vortex induced (pressure) drag by about an order of magnitude.

Recommendations

While this investigation demonstrates the potential that feedback flow control offers in terms of reducing unsteady lift and drag of a bluff body at low Reynolds numbers, it is unclear what the results of applying the control approaches employed in this research at higher Reynolds numbers will be. Unforced CFD simulations at a Reynolds

number of 160 show that the vortex induced drag portion of the overall drag increases from 16% at Re = 100 to more than 30% at Re = 160. This indicates that the same control approach at higher Reynolds numbers may yield larger decreases in drag. However, this will have to be investigated in detail in future research.
Additionally, we still have to close the feedback loop in our experimental investigation, the results of which we intend to present at one of the winter conferences. This will be the ultimate test for the applicability of the simulation results to real life experiments.

Acknowledgments

The authors would like to acknowledge funding for this research from the Air Force Office of Scientific Research, program monitor Dr. Belinda King. We would also like to acknowledge the fruitful discussions and information exchange with Gilead Tadmor and Bernd Noack.

References

1 Williamson, C.H.K., "Vortex Dynamics in the Cylinder Wake", *Ann. Rev. Fluid Mech.*, 1996, 28:477-539

2 Roussopoulos, K., "Feedback control of vortex shedding at low Reynolds numbers", *Journal of Fluid Mechanics*, Vol. 248, 1993, pp. 267-296.

3 Park, D. S., Ladd, D. M., and Hendricks, E. W., "Feedback control of von Kármán vortex shedding behind a cylinder at low Reynolds numbers", *Phys. Fluids*, Vo. 6, No.7, 1994, pp. 2390-2405.

4 Monkewitz, P. A., "Modeling of self-excited wake oscillations by amplitude equations", *Experimental Thermal and Fluid Science*, Vol. 12, 1996, pp. 175-183.

5 Blevins, R., "Flow Induced Vibration", 2nd Edition, Van Nostrand Reinhold, 1990, pp. 54-58.

6 Koopmann, G., "The Vortex Wakes of Vibrating Cylinders at Low Reynolds Numbers", *Journal of Fluid Mechanics*, Vol. 28 Part 3, 1967, pp. 501-512.

7 Min, C., Choi, H., "Suboptimal Feedback Control of Vortex Shedding at low Reynolds Numbers", *Journal of Fluid Mechanics*, Vol. 401, 1999, pp. 123-156.

8 Gillies, E. A., "Low-dimensional characterization and control of non-linear wake flows", PhD. Dissertation, University of Glasgow, Scotland, June 1995.

9 Li, F. and Aubry, N., "Reactive flow control for a wake flow based on a reduced model", AIAA Paper 2000-2531, Fluids 2000 Conference and Exhibit, Denver, CO, June 19-22, 2000

10 Bewley, T. and Trenchea, C., "Noncooperative Optimization of Controls for Time-Periodic Navier-Stokes Systems (Invited)", AIAA Paper 2002-2754, 3rd Theoretical Fluid Mechanics Meeting, St. Louis, 2002.

11 Gillies, E. A., "Low-dimensional control of the cylinder wake", *Journal of Fluid Mechanics*, Vol. 371, 1998, pp. 157-178.

12 Cohen, K., Siegel, S., McLaughlin, T., Gillies, E., "Feedback Control of a Cylinder Wake Low Dimensional Model", accepted for publication in the AIAA Journal

13 Oertel, H. Jr., "Wakes Behind Blunt Bodies", *Annual Review of Fluid Mechanics*, Vol. 22, 1990, pp. 539-564.

14 Panton, R.L., "Incompressible Flow", 2nd Edition, John Wiley & Sons, New York, 1996, pp. 384-400.

15 Holmes, P., Lumley, J. L., and Berkooz, G., "Turbulence, Coherent Structures, Dynamical Systems and Symmetry", Cambridge University Press, Cambridge, Great Britain, 1996, pp. 86-127.

16 Sirovich, L., "Turbulence and the Dynamics of Coherent Structures Part I: Coherent Structures", *Quarterly of Applied Mathematics*, Vol. 45, No. 3, 1987, pp. 561-571.

17 Smith, D. R., Siegel, S., and McLaughlin T., "Modeling of the wake Behind a Circular Cylinder Undergoing Rotational Oscillation", AIAA Paper 2002-3066, June 2002.

18 Noack, B.R., Afanasiev, K., Morzynski, M. and Thiele, F., "A hierarchy of low-dimensional models for the transient and post-transient cylinder wake', accepted for publication in *J. Fluid Mechanics*, 2003.

19 Ahlborn, B., Seto, M., Noack, B., "On drag, strouhal number and vortex street structure", accepted for publication in *J. Fluid Mechanics*, 2003.

20 Gerhard, J., Pastoor, M., King, R., Noack, B., Dillman, A., Morzynski, M., Tadmor, G., "Model-based control of vortex shedding using low-dimensional Galerkin models" AIAA Paper 2003-4262, June 2003.